sciendo

POLISH MARITIME RESEARCH 1 (117) 2023 Vol. 30; pp. 145-155
10.2478/pomr-2023-0015

INVESTIGATING THE HARBOUR BASIN TRANQUILLITY IN THE GENAVEH PORT DEVELOPMENT PLAN

Mahdi Bandizadeh Sharif [1]
Amir Hossein Gorbanpour [2]
Hassan Ghassemi [1,3*]
Guanghua He [3]

[1] Department of Maritime Engineering, Amirkabir University of Technology, Tehran, Iran
[2] Department of Civil Engineering, University of Tehran, Tehran, Iran
[3] International School of Ocean Science and Engineering, Harbin Institute of Technology, Weihai, China

* Corresponding author: *Gasemi@aut.ac.ir (Hassan Ghassemi)*

ABSTRACT

The Genaveh commercial port was placed on the agenda of the Iranian PMO (ports and maritime organization) to consider economic, commercial and residential development in Bushehr province and specifically in Genaveh city. In order to increase the water capacity of the port, it is necessary to build a new harbour basin for exploitation and commercial purposes at a depth of 5 to 6 meters by extending the existing jetties arms in front of the port. This research aims to investigate the harbour basin's tranquillity for providing vessels with safe berthing. For this purpose, three modules, namely the flow model (FM), spectral wave (SW) and Boussinesq waves model (BW) from the MIKE 21 software package, were utilized. According to the monitoring data, which is provided by the Iranian PMO, the harbour basin's tranquillity based on the prevailing wave directions was investigated. Based on the diffraction graph in the harbour basin, the results showed that, according to the percentage of permissible diffraction recommended by different valid regulations, there is a need to modify the geometry of the breakwater arms to increase the harbour basin's tranquillity at the port in the development plan.

Keywords: harbour basin tranquillity, Genaveh Port, Boussinesq wave model, diffraction, breakwater, numerical modelling

INTRODUCTION

Port development can be accomplished by constructing a new harbour basin or expanding the existing basin, where the purpose is usually to increase the marine capacity and upgrade port operations, which both have a direct impact on the regional economy [1]. To increase the port capacity, it is necessary to build a harbour basin that is surrounded by an artificial breakwater to provide suitable tranquillity at the harbour basin [2, 3]. The important tasks of the harbour basin are to create a safe berthing and anchorage for vessels, provide a platform to transfer passengers safely between vessels and land and improve the efficiency of vessel transportation by reducing the waiting time of vessels at the port [4, 5]. The most important issue in the construction of an artificial harbour basin to increase the port capacity is the location of the breakwater arms that form the basin. The location and width of the harbour basin mouth are important, in addition to serving the incoming and outgoing vessels, to provide the tranquillity necessary for the safe berthing and anchorage of vessels in the port [6, 7]. While wave agitation cannot affect bigger vessels, the same wave agitation encountering small vessels can cause their violent movement, so determining the target vessel of the port is necessary [8]. In the most recent research, different proposed methods based on the finite difference method are used to calculate harbour tranquillity [9-13]. The most common method used to investigate the tranquillity of harbour basins is the Boussinesq waves model, which employs the finite element method [14, 15].

In this model, the impact of the input parameters such as the hydrodynamic conditions of the area and the placement of the harbour basin mouth affects the level of calmness in the basin. These studies showed the diffraction patterns of waves inside the harbour basin by determining the phenomena of the diffraction, reflection and energy loss when the waves hit the rubble mound breakwater layers. The design of the model of wave propagation and penetration into the harbour basin has been performed according to the placement of the breakwater arms and the probable and effective directions of the waves. To increase the speed of the model execution, the areas where the wave characteristics and the wave diffraction pattern are not needed are defined in [7, 16-20]. In this study, to increase the capacity of Genaveh port, which is facing a number of problems, research was done to minimize the obstacles to the development of the port. Researchers showed that several factors influence the characteristic conditions in Genaveh port, such as the Dareh Gap River, which is located at the longitude of 50°31′57.53″E and latitude of 29°32′3.27″N, and flows into the Persian Gulf where it is located southeast of Genaveh port. To reduce the sediment transport from the Dareh Gap River to the harbour basin, two jetty structures were constructed at the depth of 3.5 meters from the chart datum level. Nevertheless, the Dareh Gap River transfers the sedimentation mostly at the harbour basin mouth. The structures have reduced the dredging time of the port and consequently decreased the operating costs. According to the proposed pattern, the shelter provided by the harbour basin will be investigated and it will be determined whether the placement of the breakwater arms can provide the allowable calmness inside the harbour basin or not.

MATERIALS AND METHODS

The flow model (FM), spectral wave (SW) and Boussinesq wave (BW) modules from the MIKE 21 software are the main computing components used in this study. The FM module comprises different models, but in this research the hydrodynamic model (HD) was selected, which calculates the water surface changes and flows in response to a variety of forcing functions, comprising wind shear stress, bed shear stress and wave radiation stress from the SW module. The SW module calculates the growth, decay and transformation of waves caused by the wind offshore and onshore, combined with current and water level changes at the same time from the HD module, and the BW module is a numerical model for calculation and analysis of short- and long-period waves in ports, harbours and coastal areas [21-26].

FM MODULE (HD MODEL)

The HD module includes a continuity equation, horizontal momentum equation, temperature, distributions of salt, and density terms and a variety of forcing and boundary conditions. The spatial discretization of the governing equation is done utilizing the finite volume method (FVM). The model simulation is based on two-dimensional Reynolds averaged Navier–Stokes (RANS) equations. The local continuity and other equations are written as:

$$\frac{\partial u}{\partial x} + \frac{\partial v}{\partial y} + \frac{\partial w}{\partial z} = S \tag{1}$$

$$\frac{\partial u}{\partial t} + \frac{\partial u^2}{\partial x} + \frac{\partial vu}{\partial y} + \frac{\partial wu}{\partial z} = f_v - g\frac{\partial \eta}{\partial x} - \frac{1}{\rho_0}\frac{\partial P_a}{\partial x} - \frac{1}{\rho_0}\int_z^{\eta}\frac{\partial \rho}{\partial x}\,dz + F_u + \frac{\partial}{\partial z}\left(v_t\frac{\partial u}{\partial z}\right) + u_s S \tag{2}$$

$$\frac{\partial v}{\partial t} + \frac{\partial v^2}{\partial y} + \frac{\partial uv}{\partial x} + \frac{\partial wv}{\partial z} = f_u - g\frac{\partial \eta}{\partial y} - \frac{1}{\rho_0}\frac{\partial P_a}{\partial y} - \frac{g}{\rho_0}\int_z^{\eta}\frac{\partial \rho}{\partial y}\,dz + F_v + \frac{\partial}{\partial z}\left(v_t\frac{\partial v}{\partial z}\right) + v_s S \tag{3}$$

$$\frac{\partial T}{\partial t} + \frac{\partial uT}{\partial x} + \frac{\partial vT}{\partial y} + \frac{\partial wT}{\partial z} = F_t + \frac{\partial}{\partial z}\left(D_v\frac{\partial T}{\partial z}\right) + \hat{H} + T_s S \tag{4}$$

$$\frac{\partial T}{\partial t} + \frac{\partial us}{\partial x} + \frac{\partial vs}{\partial y} + \frac{\partial ws}{\partial z} = F_s + \frac{\partial}{\partial z}\left(D_v\frac{\partial s}{\partial z}\right) + s_s S \tag{5}$$

$$\left(F_r \cdot F_s\right) = \left[\frac{\partial}{\partial x}\left(D_h\frac{\partial}{\partial x}\right) + \frac{\partial}{\partial y}\left(D_h\frac{\partial}{\partial y}\right)\right]\left(T \cdot s\right) \tag{6}$$

where u, v and w are the velocity components in the x, y and z direction in the Cartesian coordinates; t is time (s); $f=2\Omega \sin\phi$ is the Coriolis force (Ω is the angular rate of revolution and ϕ is the geographic latitude); g is the gravitational acceleration; ρ is the fluid density; P_a is the pressure; T and s are the temperature and salinity; D_v is the vertical turbulent (eddy) diffusion coefficient; $\hat{H}$ is a source term due to heat exchange with the atmosphere; S is the magnitude of discharge due to point sources; T_S and S_S are the temperature and salinity of the source; F_T, F_S are horizontal diffusion terms and D_h represents the horizontal diffusion coefficient.

SW MODULE

The SW module calculates the growth, decay and transformation of wind-generated waves and swells in offshore and coastal areas. Like the HD module, FVM is used for the discretization of the governing equation in geographical and spectral space. This module includes the following physical phenomena: (a) generation and growth of waves by wind action; (b) wave-wave, wave-current and quadruplet-wave interaction (c) loss due to white-capping, bed friction and wave breaking; (d) diffraction, refraction and shoaling in shallow water, and (e) effect of time-varying water depth. The wave action conservation equation is the governing equation, which will be used in either Cartesian or spherical coordinates in the fully spectral formulation. The equations for the fully spectral formulation in horizontal Cartesian coordinates are as follows:

$$\frac{\partial N}{\partial t} + \nabla \cdot (\bar{v}N) = \frac{S}{\sigma} \tag{7}$$

$$\left(c_x \cdot c_y\right) = \frac{d\bar{x}}{dt} = \bar{c}_g + \bar{U} \tag{8}$$

$$c_\sigma = \frac{d\sigma}{dt} = \frac{d\sigma}{\partial d}\left\{\frac{\partial d}{\partial t} + \bar{U}\cdot\nabla_{\bar{x}} d\right\} - c_g \bar{k}\frac{\partial \bar{U}}{\partial s} \quad (9)$$

$$c_\theta = \frac{d\theta}{dt} = -\frac{1}{k}\left\{\frac{\partial \sigma}{\partial d}\frac{\partial d}{\partial m} + \bar{k}\frac{\partial \bar{U}}{\partial m}\right\} \quad (10)$$

$$c_g = \frac{d\sigma}{dk} \quad (11)$$

in which $N(x, \sigma, \theta, t)$ represents the action density which is equal to E/σ; t is the time; ∇ is the four-dimensional differential operator in the x direction; $v = (c_x \cdot c_y, c_\theta \cdot c_\sigma)$ represents the propagation velocity of a wave group in the four-dimensional phase space x, y, σ and θ; $x = (x, y)$ are the Cartesian coordinates; S is the source term for the energy balance equation; s is the space coordinate in wave direction θ; m is a coordinate perpendicular to s. ∇_x is the two-dimensional differential operator in the x-space.

BW MODULE

MIKE 21-BW was used to calculate the pattern of the diffraction inside the basin. This module can examine the wave propagation pattern by considering the simultaneous effects of phenomena such as shoaling, refraction, diffraction, bottom friction, partial reflection and transmission, frequency spreading and directional spreading. In this model, the Boussinesq equations are based on the assumption of being incomparable and inviscid fluid were used to determine the diffraction coefficient numerically inside the basin. The governing equations are expressed as follows:

$$n\frac{\partial s}{\partial t} + \frac{\partial P}{\partial x} + \frac{\partial q}{\partial y} = 0 \quad (12)$$

$$n\frac{\partial P}{\partial t} + \frac{\partial}{\partial x}\left(\frac{P^2}{h}\right) + \frac{\partial}{\partial y}\left(\frac{Pq}{h}\right) + \frac{\partial R_{xx}}{\partial x} + \frac{\partial R_{xy}}{\partial x} + n^2 gh\frac{\partial S}{\partial x} + n^2 P\left(\alpha + \beta\sqrt{\frac{P^2}{h^2} + \frac{q^2}{h^2}}\right) + \frac{gp\sqrt{P^2+q^2}}{h^2 C^2} + n\psi_1\psi_1 = 0 \quad (13)$$

$$n\frac{\partial P}{\partial t} + \frac{\partial}{\partial y}\left(\frac{P^2}{h}\right) + \frac{\partial}{\partial x}\left(\frac{Pq}{h}\right) + \frac{\partial R_{yy}}{\partial y} + \frac{\partial R_{xy}}{\partial y} + n^2 gh\frac{\partial S}{\partial y} + n^2 P\left(\alpha + \beta\sqrt{\frac{P^2}{h^2} + \frac{q^2}{h^2}}\right) + \frac{gp\sqrt{P^2+q^2}}{h^2 C^2} + n\psi_2\psi_2 = 0 \quad (14)$$

$$\psi_1 = -\left(B + \frac{1}{3}\right)d^2\left(P_{xxt} + q_{xyt}\right) - nBgd^3\left(S_{xxx} + S_{xyy}\right) - dd_x\left(\frac{1}{3}P_{xt} + \frac{1}{6}q_{yt} + nBgd\left(2S_{xx} + S_{yy}\right)\right) - dd_y\left(\frac{1}{6}q_{xt} + nBgdS_{xy}\right) \quad (15)$$

$$\psi_2 = -\left(B + \frac{1}{3}\right)d^2\left(q_{yyt} + P_{xyt}\right) - nBgd^3\left(S_{yyy} + S_{xxy}\right) - dd_y\left(\frac{1}{3}q_{yt} + \frac{1}{6}P_{xt} + nBgd\left(2S_{yy} + S_{xx}\right)\right) - dd_x\left(\frac{1}{6}P_{yt} + nBgdS_{xy}\right) \quad (16)$$

$$R_{xx} = -\frac{\delta}{1-\frac{\delta}{h}}\left(C_x - \frac{P}{h}\right)^2 \quad (17)$$

$$R_{xy} = -\frac{\delta}{1-\frac{\delta}{h}}\left(C_x - \frac{P}{h}\right)\left(C_y - \frac{q}{h}\right) \quad (18)$$

$$R_{yy} = -\frac{\delta}{1-\frac{\delta}{h}}\left(C_y - \frac{q}{h}\right)^2 \quad (19)$$

where P is the flux density in the x-direction ($m^3/m/s$), q represents the flux density in the y-direction ($m^3/m/s$), x and y are the Cartesian coordinates (m), h and d are the total water depth and still water depth (m) respectively, n is the porosity coefficient, C is the Chezy resistance number ($\sqrt{m}/s$), α and β represent the resistance coefficient for laminar and turbulent flow in porous media, S is the water level compared to the base level (m), ψ_1 and ψ_2 are the dispersive Boussinesq terms, and R_{xx}, R_{xy} and R_{yy} are the excess momenta from surface rollers.

STUDY AREA

Genaveh port is a commercial fishing port on the northern coast of the Persian Gulf, as displayed in Fig. 1a. This port connects with Imam Hassan port from the northwest, which is at the longitude of 50°15′39″ E and latitude of 29°50′16″ N, and Bushehr city from the northeast and the Persian Gulf from the west. The port city of Genaveh is located in the northern part of the Persian Gulf at a longitude of 50°31′ E and latitude of 29°34′N. According to the hydrodynamic condition and sediment transport in the region, the first proposed pattern of the harbour basin is based on the existing basin as can be seen in Fig. 1b. Table 1 gives the length of the existing northern and southern jetties and the new pattern of the breakwater arms.

Fig. 1. (a) Location of Genaveh port, (b) the first pattern

Tab. 1. The length of the breakwater arms of the development plan

Pattern	Northern arm (m)	Southern arm (m)
Existung	1000	1000
First proposal	620	1870

HYDRODYNAMIC STUDIES

To check the tranquillity inside the harbour basin, the propagation of waves in the local area will be investigated, based on the data received from the Iranian PMO and the hydrodynamic studies carried out in this research. Wave forecasting information in the area of the Bushehr province

coasts was obtained from the monitoring and simulation of the waves carried out over a period of 26 years (from 01/01/1983 to 01/06/2009) by the PMO. The MIKE-SW module was utilized in this research to generate waves. The wave information in this study was prepared and presented with a time step of 1 hour. The information related to the waves of this statistical source is provided at the longitude of 50.40°and latitude of 29.60°N in front of the port site at a depth of 23 meters. Based on this data, about 75% of the time the wave height is less than 0.5 meters, and the maximum wave height is 2.49 meters in the direction of 166 degrees. Based on the wave rose, the predominant direction of the waves is from the northwest to the southeast direction, as displayed in Fig. 2 [27].

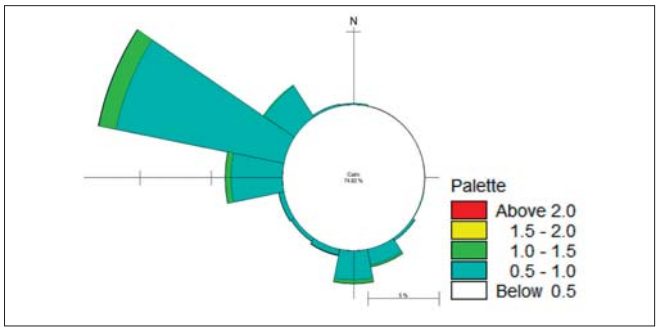

Fig. 2. Wave rose at the depth of 23 meters during 1983-2009

To determine the annual wave rose in front of the port, the base year concept is defined. The selection of the base year is based on the way that the characteristics of the waves in that year are the most consistent and match the characteristics of the waves of the entire period. The wave statistics of the region for the 26 years from 1983 to 2009 were defined. Each wave rose that best matches the 26-year wave rose will be selected. Based on Fig. 3 and Fig. 4 the 2005 wave rose is chosen as the base year of calculation as it shows the best compatibility and match with the 26-year wave rose. Therefore, the wave rose of 2005 was chosen for the base year calculation, as shown in Fig. 5.

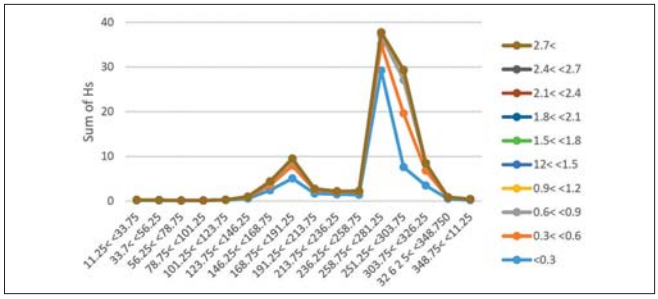

Fig. 3. The scatter data graph of the 26-year wave data

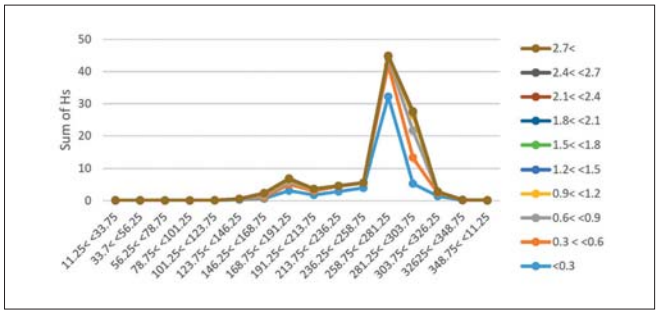

Fig. 4. The scatter data graph of the 2005 wave data

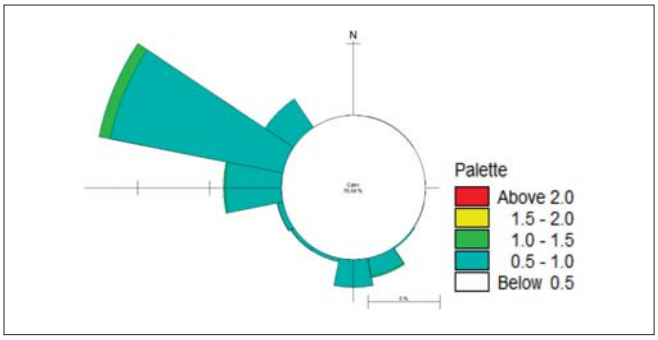

Fig. 5. Wave rose at the depth of 10 meters, 2005

To calculate the significant wave height and the wave speed at the harbour basin, the characteristics of the design waves and wind at the depth of 23 meters in front of the port are presented in Table 2. According to the data shown in the table, the 100-year wave height occurs in the direction of 157.5°, which is equal to 3.91 meters. The prevailing 100-year wind speed occurs in the direction of 315°, equal to 18.45 m/s.

Tab. 2. Design wave and wind in the research area

Direction (deg.)	Return period (year)	Wave		Wind speed (m/s)	Wave distribution	Wind distribution
		H_s(m)	T_p(s)			
157.5	1	1.02	3.87	6.96	LP2/ MOM	LP3/ MOM/ Log
	5	1.66	4.04	13.73		
	10	2.02	4.11	14.70		
	50	3.20	4.27	16.68		
	100	3.91	4.35	17.47		
180	1	1.328	4.76	5.14	TGUM/ ML	TGUM/ ML
	5	1.741	4.95	11.97		
	10	1.922	5.02	12.90		
	50	2.341	5.16	14.86		
	100	2.522	5.22	15.66		
270	1	1.003	4.71	6.22	GAM/ MOM	GAM/ MOM
	5	1.448	5.04	12.15		
	10	1.541	5.09	13.05		
	50	1.741	5.21	14.94		
	100	1.825	5.26	15.72		
292.5	1	1.085	4.39	8.30	GAM/ MOM	GAM/ MOM
	5	1.656	4.81	12.38		
	10	1.779	4.89	13.00		
	50	2.051	5.04	14.25		
	100	2.166	5.11	14.75		
315	1	1	3.81	11.62	GAM/ MOM	LP2/ MOM
	5	1.205	3.96	15.69		
	10	1.299	4.02	16.41		
	50	1.517	4.15	17.87		
	100	1.613	4.21	18.45		

ALLOWABLE HS AT THE BASIN

According to the technical standards and commentaries for port and harbour facilities in the Japan guide, the maximum

allowable significant wave height at the berthing area of vessels based on their gross tonnage (GT) is stated in Table 3. Based on this reference, it is recommended that the harbour basin and the place of servicing vessels (piers) should be calm at least 97.5% of all days of the year and have favorable conditions for the mooring and parking of vessels. According to the value mentioned in Table 3, the maximum wave height of 0.5 meters is considered the tranquillity criterion of this harbour by the Overseas Coastal Area Development Institute of Japan.

Tab. 3. The maximum Hs allowed for servicing the vessel

Type of vessel	Gross tonnage (GT)	Permitted *Hs* for serving the vessel
Small	Less than 500 tons	0.3 meters
Medium and large	Between 500 and 50000 tons	0.5 meters
Very big	More than 50,000 tons 620	0.7 – 1.5 meters

INPUT DATA OF BW MODULE

According to the wave rose information, the effective directions of 157.5°, 180°, 270°, 292.5° and 315° (relative to true north) were propagated towards the port. It should be noted that, because of the lack of disturbance in the port due to the propagation of waves from other directions, only the propagation of the mentioned wave directions is sufficient. The input wave data is defined as a wave spectrum based on the JONSWAP spectrum. There are 5 porous layers in front of the pier structures and 20 sponge layers. The porosity coefficient is a function of the type of structure (stone breakwater, wall pier, pile pier and deck, etc.), its reflection coefficient, the water depth at the base of the structure and the height and period of the wave at the location of the structure. Based on the aforementioned explanations, it is necessary to estimate the value of the porosity coefficient using previous experience and engineering judgment and then after one or more executions, the final value of the porosity coefficient is determined. The grid spacing of the model is set to 4 meters. Also, assuming that the wave distribution pattern inside the harbour basin is approximately a linear function of the incoming wave height (in other words, the diffraction coefficients inside the harbour basin remain almost constant for different wave heights), the investigation of the phenomenon of diffraction inside the basin for the wave is done with a unit height (1 m). Fig. 6a shows the bathymetric model used in the modelling, and the positions of the porous and spongy layers are displayed in Fig. 6b and Fig. 6c, respectively. Fig. 6b shows the position of applying the porous layer at about the level of the water surface and the breakwaters. The porous layer is considered as 5 layers with values of 0.66 outside and 0.56 inside the harbour basin. In Fig. 6c, in the areas where the reflection of the propagated waves is not compatible with the physical realities of the phenomenon (for example, in the boundaries of the model), the sponge layer technique was used [28].

RESULTS AND DISCUSSION

HD AND SW RESULTS

Wave propagation with a return period of 100 years from the directions of 157.5°, 180°, of 270°, 292.5° and 315° are shown in Fig. 7. It can be seen in the 270°, 292.5° and 315° directions that the breakwater arms or the harbour basin mouth cannot provide

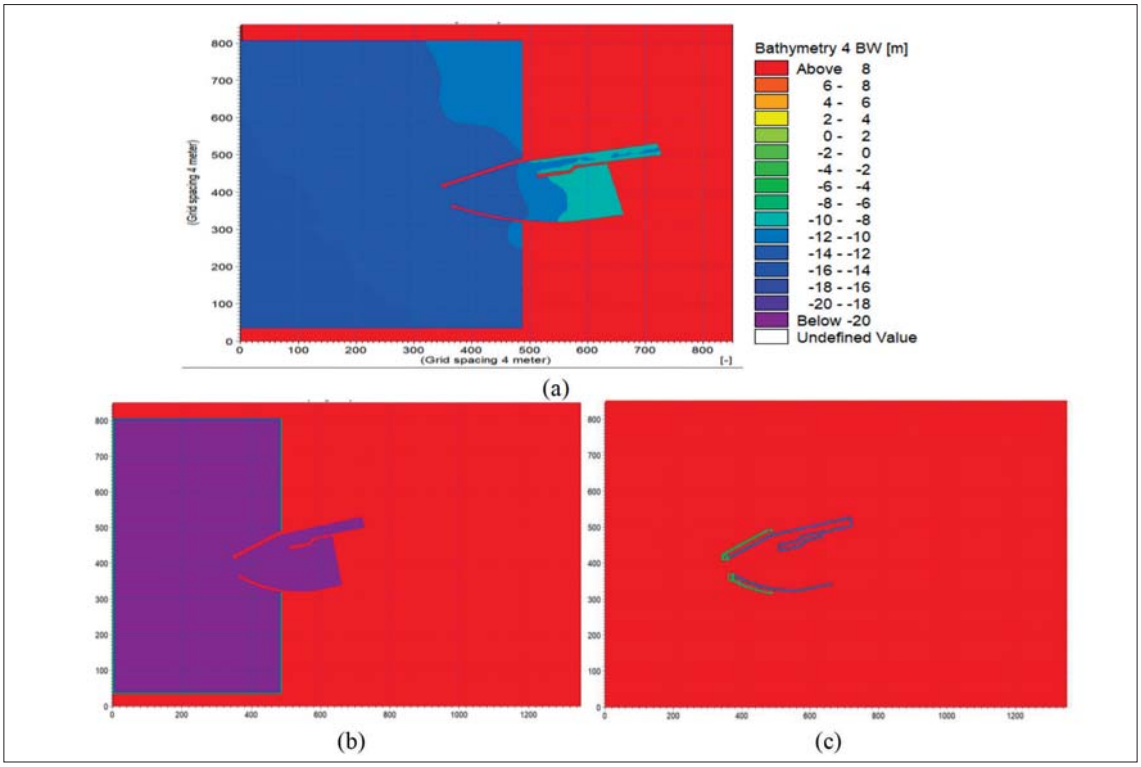

Fig. 6. The initial BW input data: (a) bathymetry model used in modelling, (b) sponge layer used in modelling, (c) porosity layer used in modelling

standard tranquillity in the basin. The significant wave height inside the basin illustrated in Fig. 8 and Fig. 9 displays the wave speed inside the basin in the dominant directions. Based on the results, the significant wave height and wave speed in the harbour basin mouth are about 3 m and 2.5 m/s, respectively, which shows that this pattern is not suitable for providing tranquillity in the harbour basin. In addition, based on the contour of H_s and the wave speed inside the basin, this placement of the breakwater arms or the harbour basin mouth causes disturbance in front of the existing basin as well as difficulties for vessel movements.

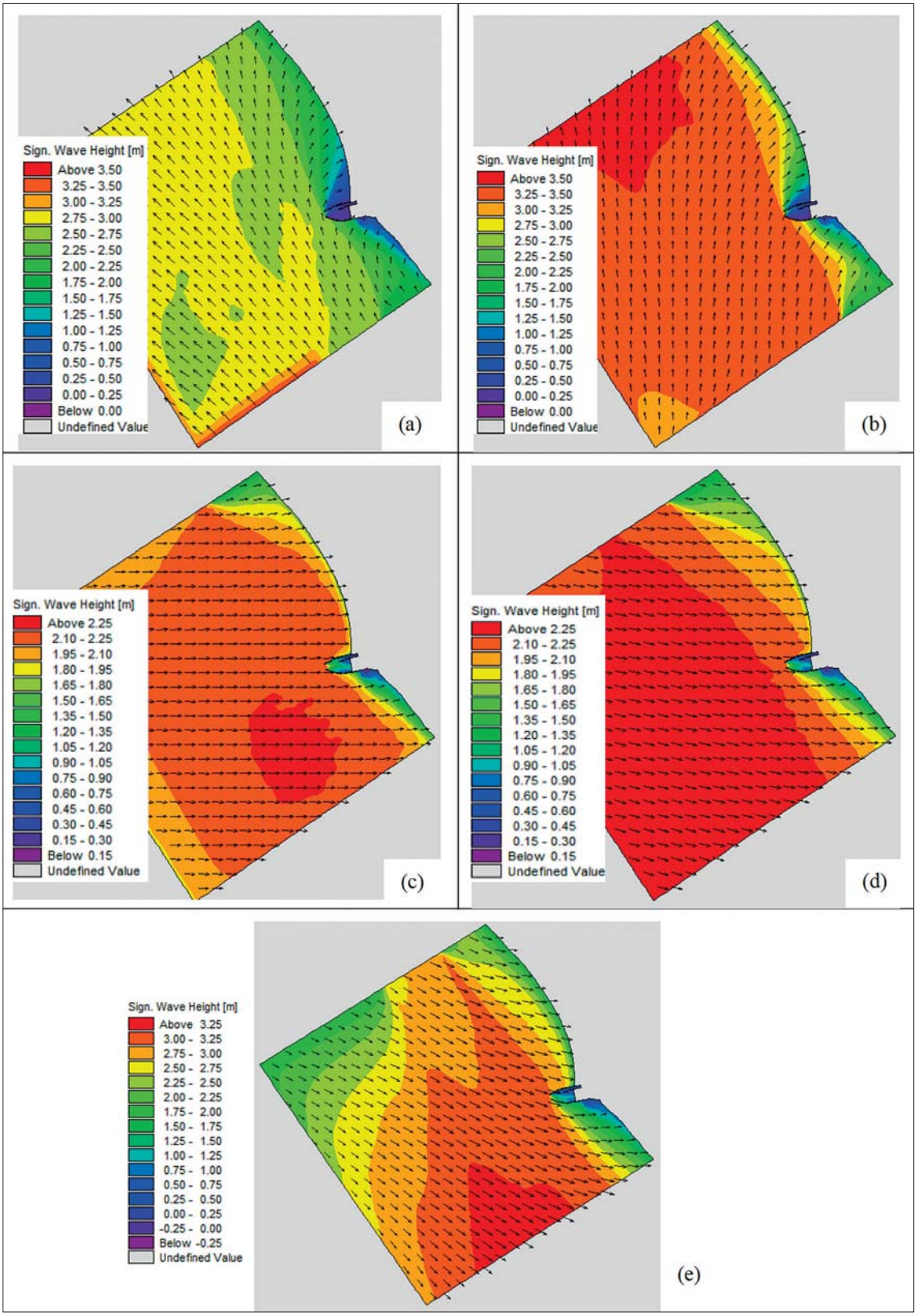

Fig. 7. Wave propagation with a return period of 100 years from the dominant directions: (a) 157.5°, (b) 180°, (c) 270°, (d) 292.5°, (e) 315°

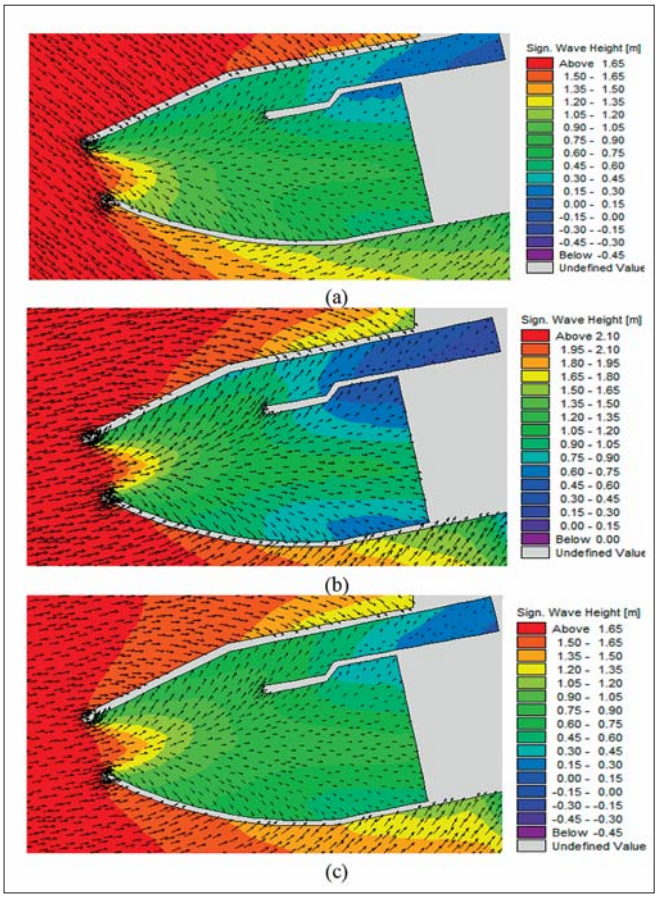

Fig. 8. Significant wave height: (a) direction of 270°, (b) 292.5°, (c) 315°

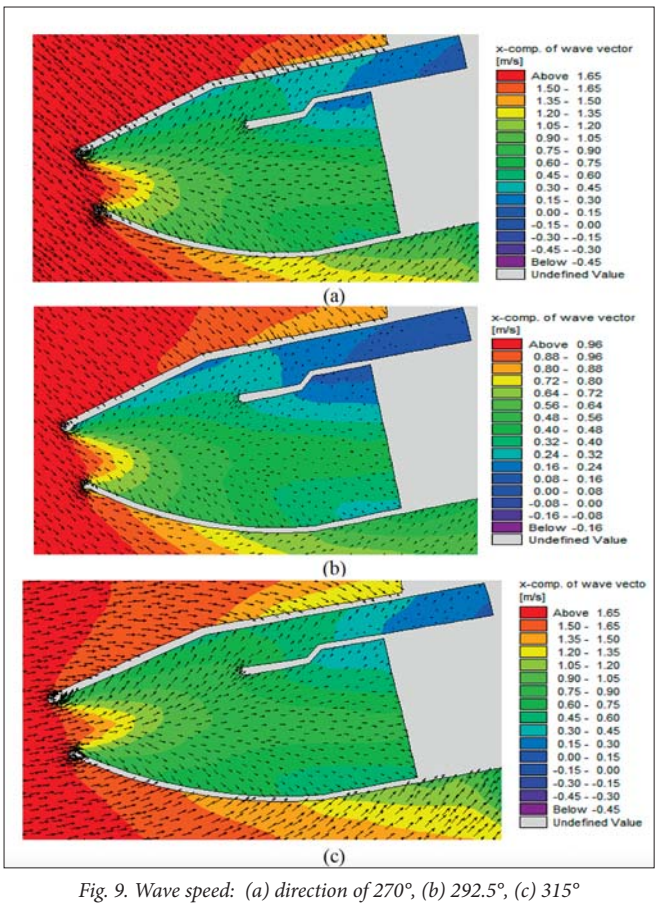

Fig. 9. Wave speed: (a) direction of 270°, (b) 292.5°, (c) 315°

The *Hs* and wave speed (S) in the X and Y directions are determined at the defined points near the first pattern breakwater arms as stated in Table 4. In the outputs with 100-year wave propagation, the hydrodynamic changes caused by the breakwater construction around the breakwater arms and near the harbour basin mouth are shown in Fig. 10. As can be seen in Table 4, at points N4 and N5, the H_s and wave speed values are the highest, which causes disturbance in the performance of the port.

Tab. 4. Hydrodynamic characteristics at the defined point in the first pattern

Name	X (northing)	Y (easting)	H_S max (m)	S_X max (m/s)	S_Y max (m/s)
N1	451475.74086	3269940.5481	2.8624	2.4956	0.2513
N2	451232.06014	3269857.0958	2.9293	2.5267	0.4573
N3	450998.3937	3269740.2625	2.9894	2.5410	1.0018
N4	450784.75581	3269556.6675	3.0357	2.5421	2.5527
N5	450891.57476	3269239.5487	3.0160	2.5605	2.6476
N6	451218.70777	3269092.6727	2.6033	2.2508	2.5600
N7	451532.48842	3269049.2775	2.5030	1.9995	2.4180
N8	451849.60716	3269035.9251	2.2806	1.8560	2.1433

Fig. 10. Defined points near the breakwater arms

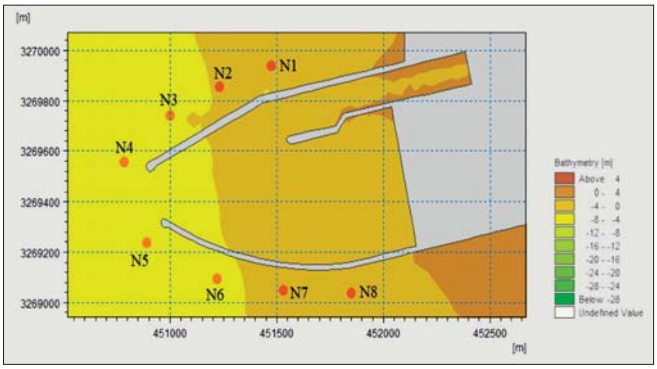

BW RESULTS

Due to the hydrodynamic conditions in the research area, there are different dominant directions. Therefore, modelling was done in the five dominant directions of 157.5°, 180°, 270°, 292.5° and 315° and the results are presented in Fig. 11. As the figure shows, due to the hydrodynamic conditions in the upstream side of the port, the wave generation lines are aligned in the dominant wave directions.

To determine the diffraction coefficient in the basin, it is necessary to extract the percentage of wave occurrences and the significant wave height along the moorings and the areas that are important for operations, in line also with the criteria provided in the regulations and valid international guidelines to obtain the diffraction distribution. Therefore, there is a need to define the specific locations in the harbour basin to calculate the percentage of disturbance at these different locations, which in Genaveh port are as shown in Fig. 12a. As can be seen, four lines were considered for the tranquillity studies. These

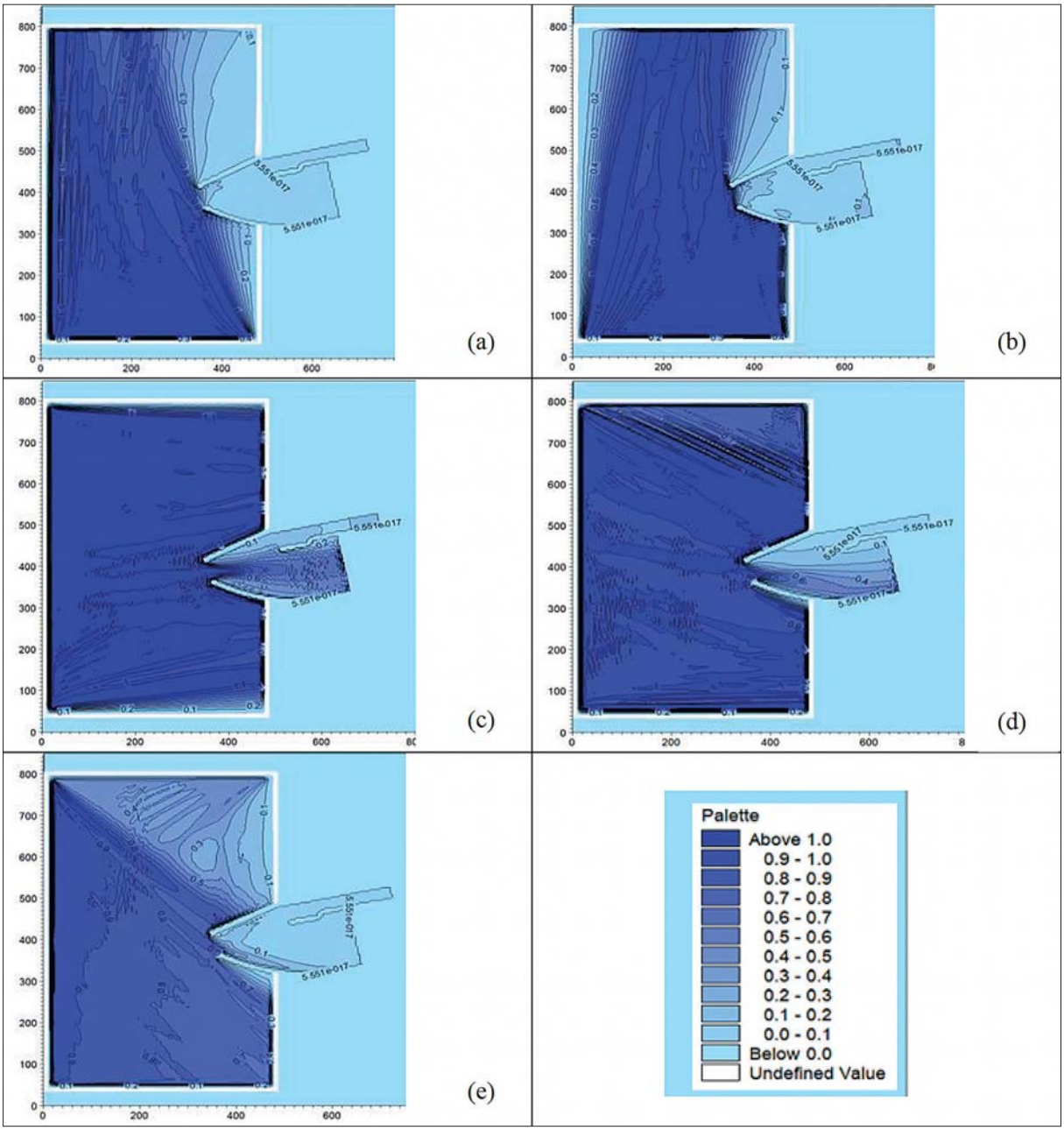

Fig. 11. Patterns of wave diffraction inside the harbour basin in the dominant directions: (a) 157.5°, (b) 180°, (c) 270°, (d) 292.5°, (e) 315°

lines are suitable for mooring and anchorage vessels inside the harbour basin. The calculated wave height ratio along the harbour moorings for the existing plan of Genaveh port is shown in Fig. 12. These figures show the ratio of the wave height at the breakwater structure to the incoming wave. In addition, increasing the wave period as expected will increase the instability of the structures.)In Fig. 12: Line 1 is blue, Line 2 is red, Line 3 is green, and Line 4 is purple).

Based on the result, the waves in the directions of 270° and 292.5° affect the tranquillity and the anchorages of the harbour basin, and their rate of occurrence during the year is more than the allowed amount. According to Fig. 12 and the allowable percentage of wave occurrence that was stated, the percentage of diffraction for the defined lines of Genaveh port is calculated in different directions, as given in Table 5.

Tab. 5. Percentage of disturbance in defined lines for different directions

Index	157.5°	180°	270°	292.5°	315°	Total (%)
The first line	0	0	0.7	1.21	0	1.91
The second line	0	0	0	0	0	0
The third line	0	0	0	0	0	0
The fourth line	0	0	0	0	0	0
Total (%)T	0	0	0.7	1.21	0	1.91

CONCLUSIONS

In this paper, the monitoring data of the Bushehr province coasts were determined as deep water base statistics, and then the wave rose for 2005 at the depth of 10 meters (as the best

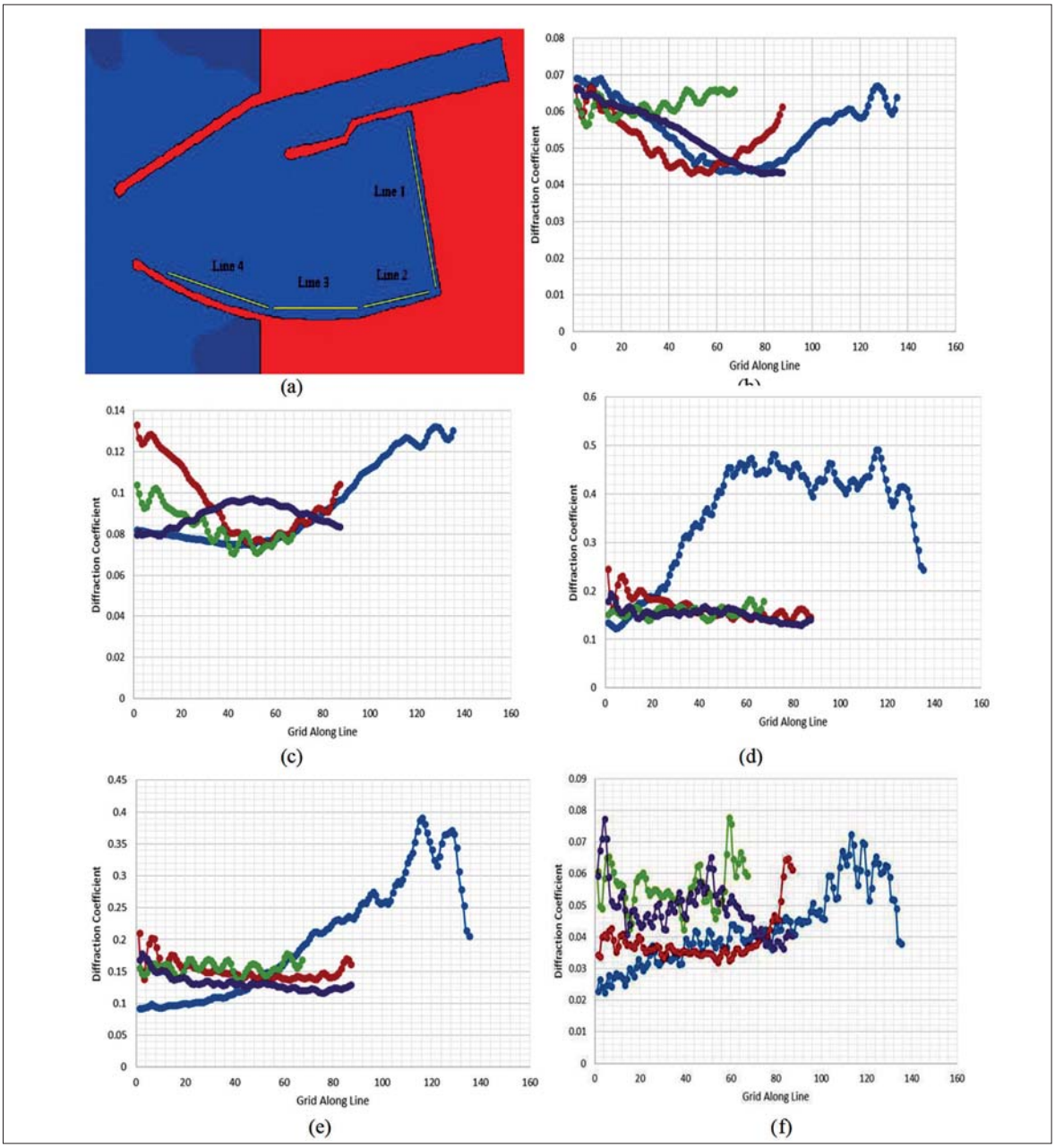

Fig. 12. Changes in the diffraction coefficient at the defined lines: (a) specific locations inside the harbour basin, (b) in the direction of 157.5°, (c) 180°, (d) 270°, (e) 292.5°, (f) 315°

match with the 26-year wave rose) was chosen as the base year of calculation. The wave propagation model was defined in the main directions of 157.5, 180, 270, 292.5 and 315 degrees. Based on the hydrodynamic results, the significant wave height and wave speed in the harbour basin mouth are about 3 m and 2.5 m/s, respectively, and the mentioned characteristics inside the basin are higher than the allowable and standard values, which shows that this pattern is not suitable for providing tranquillity in the harbour basin. In addition, in the BW model, a wave penetration model for the wave with unit height was implemented to investigate the tranquillity conditions inside the existing harbour basin and the new harbour basin. The results showed that the diffraction coefficients and disturbance at the defined lines in the harbour basin were not in the allowable range, which determined that the breakwater arms placement cannot provide suitable tranquillity inside the basin. Therefore, according to the HD, SW and BW results, the location of the breakwater arms, or in other words the harbour basin mouth, cannot provide the required tranquillity at the basin, so the geometry of the breakwater arms needs to be modified to increase the harbour basin tranquillity at the port for the development plan.

REFERENCES

1. G.P.Tsinker, "Port planning," in *Port engineering: planning, construction, maintenance, and security*, pp. 7-64, 2004.

2. M. Luo, L. Liu, and F. Gao, "Post-entry container port capacity expansion," *Transportation Research Part B: Methodological*,

vol. 46, no. 1, pp. 120-138, 2012, https://doi.org/ 10.1016/ j.trb.2011.09.001

3. K. H. Ryu, W. M. Jeong, J.-E. Oh, W.-D. Baek, and Y. S. Chang, "Wave Height Reduction Inside Pohang New Port, Korea, Due to the Construction of a Detached Breakwater," *Journal of Marine Science and Engineering*, vol. 10, no. 10, p. 1537, 2022, https://doi.org/10.3390/jmse10101537

4. Y. Goda, *Random seas and design of maritime structures*. World Scientific Publishing, 2010.

5. X. Zhang, J. Lin, Z. Guo, and T. Liu, "Vessel transportation scheduling optimization based on channel–berth coordination," *Ocean Engineering*, vol. 112, pp. 145-152, 2016, https://doi.org/10.1016/j.oceaneng.2015.12.011

6. M. Kankal, and Ö. Yüksek, "Artificial neural network approach for assessing harbor tranquility: The case of Trabzon Yacht Harbor, Turkey," *Applied Ocean Research*, vol. 38, pp. 23-31, 2012, https://doi.org/10.1016/j.apor.2012.05.009

7. J. K. Panigrahi, C. Padhy, and A. Murty, "Inner harbour wave agitation using Boussinesq wave model," *International Journal of Naval Architecture and Ocean Engineering*, vol. 7, no. 1, pp. 70-86, 2015, https://doi.org/10.2478/IJNAOE-2015-0006

8. D. González-Marco, J. P. Sierra, O. F. de Ybarra, and A. Sánchez-Arcilla, "Implications of long waves in harbor management: The Gijón port case study," *Ocean & Coastal Management*, vol. 51, no. 2, pp. 180-201, 2008, https://doi.org/10.1016/j.ocecoaman.2007.04.001

9. M. B. Abbott, A. D. McCowan, and I. R. Warren, "Accuracy of short-wave numerical models," *Journal of Hydraulic Engineering*, vol. 110, no. 10, pp. 1287-1301, 1984, https://doi.org/ 10.1061/ (ASCE)0733-9429(1984)110:10(1287)

10. G. Wei, and J. T. Kirby, "Time-dependent numerical code for extended Boussinesq equations," *Journal of Waterway, Port, Coastal, and Ocean Engineering*, vol. 121, no. 5, pp. 251-261, 1995, https://doi.org/10.1061/ (ASCE)0733-950X(1995)121:5(251)

11. S. Beji, and K. Nadaoka, "A formal derivation and numerical modelling of the improved Boussinesq equations for varying depth," *Ocean Engineering*, vol. 23, no. 8, pp. 691-704, 1996, https://doi.org/10.1016/0029-8018(96)84408-8

12. K. Barve, L. Ranganath, M. Karthikeyan, S. Kori, and M. Kudale, "Wave Tranquility and Littoral Studies for Development of a Mini Fishing Harbour," *Aquatic Procedia*, vol. 4, pp. 72-78, 2015, https://doi.org/10.1016/j.aqpro.2015.02.011

13. G. Diaz-Hernandez, B. R. Fernández, E. Romano-Moreno, and J. L. Lara, "An improved model for fast and reliable harbour wave agitation assessment," *Coastal Engineering*, vol. 170, p. 104011, 2021, https://doi.org/10.1016/j.coastaleng.2021.104011

14. Y. S. Li, S.-X. Liu, O. Wai, and Y.-X. Yu, "Wave concentration by a navigation channel," *Applied Ocean Research*, vol. 22, no. 4, pp. 199-213, 2000, https://doi.org/10.1016/S0141-1187(00)00013-4

15. Y. S. Li, S.-X. Liu, Y.-X. Yu, and G.-Z. Lai, "Numerical modeling of Boussinesq equations by finite element method," *Coastal Engineering*, vol. 37, no. 2, pp. 97-122, 1999, https://doi.org/ 10.1016/S0378-3839(99)00014-9

16. S. Abohadima, and M. Isobe, "Linear and nonlinear wave diffraction using the nonlinear time dependent mild slope equations," Coastal Engineering, vol. 37, no. 2, pp. 175-192, 1999, https://doi.org/10.1016/S0378-3839(99)00020-4

17. D. R. Fuhrman, H. B. Bingham, and P. A. Madsen, "Nonlinear wave–structure interactions with a high-order Boussinesq model," *Coastal Engineering*, vol. 52, no. 8, pp. 655-672, 2005, https://doi.org/10.1016/j.coastaleng.2005.03.001

18. M. Khalifa, "Calmness study for container handling ports with open basin systems using numerical modeling," *Marine Sciences*, vol. 20, no. 1, 2009.

19. Y.-T. Kim, and J.-I. Lee, "Construction of Fishery Port Considering Harbor Calmness, Water Circulation and Stability: Case Study," *Journal of Coastal Research*, vol. 64, pp. 641-645, 2011.

20. K. Belibassakis, V. Tsoukala, and V. Katsardi, "Three-dimensional wave diffraction in the vicinity of openings in coastal structures," *Applied Ocean Research*, vol. 45, pp. 40-54, 2014, https://doi.org/10.1016/j.apor.2013.12.005

21. M. Sedigh, R. Tomlinson, N. Cartwright, and A. Etemad-Shahidi, "Numerical modelling of the Gold Coast Seaway area hydrodynamics and littoral drift," *Ocean Engineering*, vol. 121, pp. 47-61, 2016, https://doi.org/10.1016/j.oceaneng.2016.05.002

22. M. T. Tay, S. B. Mitchell, J. Chen, and J. Williams, "Numerical modelling approach for the management of seasonal influenced river channel entrance," *Ocean & Coastal Management*, vol. 130, pp. 79-94, 2016, https://doi.org/10.1016/j.ocecoaman.2016.06.004

23. D. H. Peregrine, "Long waves on a beach," *Journal of Fluid Mechanics*, vol. 27, no. 4, pp. 815-827, 1967, https://doi.org/10.1017/S0022112067002605

24. H. A. Schäffer, and P. A. Madsen, "Further enhancements of Boussinesq-type equations," *Coastal Engineering*, vol. 26, no. 1-2, pp. 1-14, 1995, https://doi.org/10.1016/0378-3839(95)00017-2

25. G. Kim, C. Lee, and K.-D. Suh, "Extended Boussinesq equations for rapidly varying topography," *Ocean Engineering*, vol. 36, no. 11, pp. 842-851, 2009, https://doi.org/10.1016/j.oceaneng .2009.05.002

26. C. Greenwood, D. Christie, V. Venugopal, J. Morrison, and A. Vogler, "Modelling performance of a small array of Wave Energy Converters: Comparison of Spectral and Boussinesq models," *Energy*, vol. 113, pp. 258-266, 2016, https://doi.org/10.1016/j.energy.2016.06.141

27. M. Moeini, A. Etemad-Shahidi, and V. Chegini, "Wave modeling and extreme value analysis off the northern coast of the Persian Gulf," *Applied Ocean Research*, vol. 32, no. 2, pp. 209-218, 2010, https://doi.org/10.1016/j.apor.2009.10.005

28. M. Guerrini, G. Bellotti, Y. Fan, and L. Franco, "Numerical modelling of long waves amplification at Marina di Carrara Harbour," *Applied Ocean Research*, vol. 48, pp. 322-330, 2014, https://doi.org/10.1016/j.apor.2014.10.002